

# Unraveling NEK4 as a Potential Drug Target in Schizophrenia and Bipolar I Disorder: A Proteomic and Genomic Approach

Chengcheng Zhang<sup>1,2,12</sup>, ZhiHui Yang<sup>3-5,12</sup>, Xiaojing Li<sup>6,11</sup>, Liansheng Zhao<sup>1</sup>, Wanjun Guo<sup>6,11</sup>, Wei Deng<sup>6,11</sup>, Qiang Wang<sup>1</sup>, Xun Hu<sup>7</sup>, Ming Li<sup>3,4,8</sup>, Pak Chung Sham<sup>8-10</sup>, Xiao Xiao<sup>\*,3,4,13,9</sup>, and Tao Li<sup>\*,2,6,11,13,8</sup>

<sup>1</sup>Mental Health Center and Psychiatric Laboratory, the State Key Laboratory of Biotherapy, West China Hospital of Sichuan University, Chengdu, Sichuan, China; <sup>2</sup>Nanhu Brain-Computer Interface Institute, Hangzhou, China; <sup>3</sup>Yunnan Key Laboratory of Animal Models and Human Disease Mechanisms, Kunming Institute of Zoology, Chinese Academy of Sciences, Kunming, Yunnan, China; <sup>4</sup>Key Laboratory of Genetic Evolution and Animal Models, Kunming Institute of Zoology, Chinese Academy of Sciences, Kunming, Yunnan, China; <sup>5</sup>Kunming College of Life Science, University of Chinese Academy of Sciences, Kunming, Yunnan, China; <sup>6</sup>Department of Neurobiology, Affiliated Mental Health Center and Hangzhou Seventh People's Hospital, Zhejiang University School of Medicine, Hangzhou, Zhejiang, China; <sup>7</sup>The Second Affiliated Hospital, Zhejiang University School of Medicine, Hangzhou, Zhejiang, China; <sup>8</sup>Department of Psychiatry, Li Ka Shing Faculty of Medicine, The University of Hong Kong, Hong Kong SAR, China; <sup>9</sup>Centre for PanorOmic Sciences, The University of Hong Kong, Hong Kong SAR, China; <sup>10</sup>State Key Laboratory of Brain and Cognitive Sciences, The University of Hong Kong, Hong Kong SAR, China; <sup>11</sup>NHC and CAMS Key Laboratory of Medical Neurobiology, MOE Frontier Science Center for Brain Science and Brain-Machine Integration, School of Brain Science and Brain Medicine, Zhejiang University, Hangzhou, Zhejiang, China

<sup>12</sup>These authors contributed equally to this work.

<sup>13</sup>Tao Li and Xiao Xiao are co-corresponding authors who jointly directed this work.

\*To whom correspondence should be addressed: Kunming Institute of Zoology, Chinese Academy of Sciences, NO. 17 Long-Xin Lu, Kunming, Yunnan 650201, P.R. China; tel: 86-871-65189508, fax: 86-871-65190162, e-mail: [xiaoxiao2@mail.kiz.ac.cn](mailto:xiaoxiao2@mail.kiz.ac.cn) (X.X.); Affiliated Mental Health Center and Hangzhou Seventh People's Hospital, Zhejiang University School of Medicine, Hangzhou, Zhejiang 310013, P.R. China; tel: 86-571-85126501, fax: 86-571-85121532, e-mail: [litaozjusc@zju.edu.cn](mailto:litaozjusc@zju.edu.cn) (T.L.)

**Background and Hypothesis:** Investigating the shared brain protein and genetic components of schizophrenia (SCZ) and bipolar I disorder (BD-I) presents a unique opportunity to understand the underlying pathophysiological processes and pinpoint potential drug targets. **Study Design:** To identify overlapping susceptibility brain proteins in SCZ and BD-I, we carried out proteome-wide association studies (PWAS) and Mendelian Randomization (MR) by integrating human brain protein quantitative trait loci with large-scale genome-wide association studies for both disorders. We utilized transcriptome-wide association studies (TWAS) to determine the consistency of mRNA-protein dysregulation in both disorders. We applied pleiotropy-informed conditional false discovery rate (pleioFDR) analysis to identify common risk genetic loci for SCZ and BD-I. Additionally, we performed a cell-type-specific analysis in the human brain to detect risk genes notably enriched in distinct brain cell types. The impact of risk gene overexpression on dendritic arborization and axon length in neurons was also examined. **Study Results:** Our PWAS identified 42 proteins associated with SCZ and

14 with BD-I, among which NEK4, HARS2, SUGP1, and DUS2 were common to both conditions. TWAS and MR analysis verified the significant risk gene *NEK4* for both SCZ and BD-I. PleioFDR analysis further supported genetic risk loci associated with *NEK4* for both conditions. The cell-type specificity analysis revealed that *NEK4* is expressed on the surface of glutamatergic neurons, and its overexpression enhances dendritic arborization and axon length in cultured primary neurons. **Conclusions:** These findings underscore a shared genetic origin for SCZ and BD-I, offering novel insights for potential therapeutic target identification.

**Keywords:** schizophrenia/bipolar I disorder/GWAS/NEK4

## Introduction

Schizophrenia (SCZ) and bipolar disorder (BD) are two common mental disorders that often lead to enduring disability and are a source of significant public health issues globally.<sup>1</sup> Both disorders are known to have considerable

genetic components, with heritability estimates ranging from 60% to 80%.<sup>2</sup> Genome-wide analyses have revealed a substantial genetic correlation between SCZ and bipolar I disorder (BD-I), the genetic overlap between SCZ and bipolar II disorder (BD-II) is somewhat less.<sup>3</sup> It's noteworthy that SCZ is largely characterized as a prototype psychotic condition with the potential for emotional instability.<sup>4</sup> In contrast, BD-I is marked by predominant manic symptoms, and delusions congruent with mania, and a significant portion of BD-I patients also display psychotic symptoms.<sup>5</sup> Despite their distinctive features, these two psychiatric disorders share several symptoms, such as psychomotor agitation. Psychomotor agitation refers to a spectrum of abnormal behaviors frequently observed in individuals with SCZ or BD-I.<sup>6,7</sup>

Therefore, elucidating the shared genetic underpinnings between SCZ and BD-I will enhance comprehension of their intersecting pathological mechanisms. Our prior work aimed to uncover these shared genetic and molecular mechanisms across psychiatric disorders and identified that the mRNA expression of several genes conferred the risk of multiple psychiatric disorders.<sup>8-10</sup> However, the neurobiological processes by which genetic diversity influences risk, on both individual and collective levels, remain largely untapped. Significant advancements in the large-scale quantification of human brain proteins, particularly in high-throughput proteome sequencing of intricate tissues, mark a significant leap forward.<sup>11,12</sup> Proteins, as the most common pharmacological targets and biomarkers, play crucial roles in cellular and biological processes and represent the end products of gene expression.<sup>13</sup> Researchers have found that psychiatric risk genetic variations affect the abundance of brain proteins, thereby identifying potentially pathogenic proteins.<sup>14-16</sup>

In the present study, we aimed to identify novel therapeutic targets for SCZ and BD-I. We began by integrating a genome-wide association study (GWAS) dataset<sup>3,17</sup> with human brain dorsolateral prefrontal cortex (DLPFC)-derived protein quantitative trait loci (pQTL),<sup>14,15</sup> using a proteome-wide association study (PWAS) framework. To validate the identified proteome-wide significant (PWS) genes, we implemented Transcriptome-Wide Association Studies (TWAS). We also conducted genome-wide Mendelian randomization (MR) analyses, integrating brain-derived molecular quantitative trait loci, including both mRNA expression and protein abundance. To further ascertain the common pathogenic genes between SCZ and BD-I, we applied pleiotropy-informed conditional false discovery rate (pleioFDR) analysis. In addition, we conducted exploratory experiments on dendritic arborization and axon length in cultured primary neurons to investigate the neurodevelopmental impact of the identified gene. Finally, we utilized the Drug-Gene Interaction Database to explore potential interactions between the identified risk protein and various pharmaceutical compounds. Our findings underscore a common

risk gene associated with both SCZ and BD-I, presenting promising avenues for future research into their mechanisms and potential therapeutic interventions.

## Methods and Materials

### GWAS Data

The genome-wide associations for SCZ were derived from the PGC3 GWAS conducted by the Schizophrenia Working Group of the Psychiatric Genomics Consortium.<sup>17</sup> This comprehensive analysis involved 69 369 patients with SCZ and 236 642 controls, collected from cohorts of European, East Asian, African-American, and Latino ancestry, resulting in the identification of 270 distinct risk loci.<sup>17</sup> The summary statistics for BD-I GWAS, which included 25 060 cases and 449 978 controls, were collected from the study by Mullins et al<sup>3</sup> drawn from 21 countries throughout Europe, North America, and Australia. For further details on these omics data, including specific information about the demographic composition of the study cohorts, we refer readers to the original publications.<sup>3,17-20</sup>

### Proteome-wide Association Studies

The ROS/MAP study, which served as the basis for our proteome-wide association studies (PWAS), analyzed human brain proteomes derived from the dorsolateral prefrontal cortex (DLPFC) of 400 adults of European descent.<sup>14,15</sup> As outlined in a previous study, of the 8356 proteins with both proteomic and genomic data, 1475 proteins exhibited associations with SNPs in 376 subjects. We carried out the PWAS using the weights (ie, protein quantitative trait loci, pQTLs) of these 1475 proteins derived from 376 individuals.<sup>18</sup> Weights used in the present analysis were derived from <https://www.synapse.org/#/Synapse: syn23627957>. Subsequently, we used FUSION<sup>18</sup> to integrate the genetic effect of diseases (SCZ or BD-I GWAS *z*-score) with the protein weights. This was achieved by calculating the linear sum of the product of *z*-score  $\times$  weight for the independent SNPs at the locus, facilitating the PWAS for both SCZ and BD-I.<sup>19</sup>

### MR Analysis

Alongside the PWAS analysis, MR was used to corroborate pathogenic proteins common to SCZ and BD-I. For this purpose, we utilized SNP data related to *cis* pQTLs and eQTLs from the DLPFC, as provided by the ROSMAP study,<sup>19,20</sup> to serve as genetic instrumental variables (exposure) in our analysis. The GWAS data were utilized as the outcome trait data in our study. The SNPs employed in the study were selected for their ability to exposures reliably ( $P < .05$ ) and independently ( $r^2 < .001$ ), and the *F*-statistics for the SNPs were greater than 10. For determining the impact of the risk allele of the instrumenting

SNP, we employed the Wald ratio method. This method calculates the log odds change in the risk of the disorders per standard deviation change in the protein and mRNA biomarker.<sup>21</sup> In instances where multiple SNP were available for a single protein or mRNA biomarker, we used a weighted mean of the ratio estimates, weighted by the inverse variance of these ratio estimates (the inverse-variance weighted technique).<sup>22</sup> Additional methods utilized included the weighted median, MR-Egger, simple mode, and weighted mode. MR estimates were generated using the “TwoSampleMR” package v0.4.26<sup>23</sup> in R 3.6.3.

#### Transcriptome-wide association studies

We performed TWAS analyses using FUSION software (<http://gusevlab.org/projects/fusion/>). This involved merging GWAS summary statistics with gene expression weights from the CommonMind dataset, which is composed of cohorts from Caucasians, African-Americans, Hispanics, and East Asians ( $N = 467$ ).<sup>24</sup> The goal was to identify genes where mRNA expression was associated with the risk of SCZ and BD-I. The fundamental approach was as follows: during transcriptome imputation, FUSION<sup>18</sup> selected the best-performing prediction model for a gene by utilizing a 5-fold cross-validation of each model, resulting in an out-of-sample  $R^2$ . Significant associations were determined using a Bonferroni-adjusted significance level of  $3.95 \times 10^{-6}$  (ie, 0.05/12 658) to account for multiple comparisons.

#### Cell-type Specificity Analysis

We scrutinized the cell-type-specific expression of the risk genes using the Cell Types database (<https://portal.brain-map.org/atlas-and-data/rnaseq>), which contains a human brain single-cell RNA-sequencing (RNA-seq) dataset.<sup>19</sup> The website details that individual cortical layers were dissected, and nuclei were dissociated and sorted from human brain tissues using NeuN as a neuronal marker. Subsequently, RNA-sequencing was performed using either SMART-Seq v4 or 10 $\times$  Genomics Chromium Single Cell 3' v3, enabling the analysis of expression in postmortem and neurosurgical donor brain nuclei. We used CELLEX (CELL-type EXpression-specificity, v1.2.1), a method for generating cell-type expression specificity (ES) profiles, to obtain gene ES values.<sup>25</sup>

#### Assessment of Druggability

Upon methodically executing the aforementioned analytical pipeline, we prioritized the identified drug targets based on the strength of their association and the evidence of their causal relationships, considering the congruity of mRNA and protein. To further ascertain whether the proteins discovered in this study might serve as therapeutic targets, we employed the Drug-Gene

Interaction Database (DGIdb 4.0) (<https://www.dgidb.org/>) to probe the interactions between the risk proteins and medications. DGIdb illuminates potentially druggable genes considering various factors, including expert curation, text mining, drug-gene interactions (sourced from DrugBank, PharmGKB, ChEMBL, Drug Target Commons, and others), gene function, and other factors.<sup>26</sup>

#### PleioFDR Analysis

We employed pleiotropy-informed conditional false discovery rate (pleioFDR) approaches<sup>27</sup> to identify genetic overlap between SCZ and BD-I via conditional FDR (condFDR) and conjunctional FDR (conjFDR) analysis. The condFDR method leverages empirical Bayes techniques, enhancing the statistical power for single-nucleotide polymorphism (SNP) detection by using auxiliary genetic information. The conjFDR was incorporated into the condFDR approach to identify shared genomic loci between SCZ and BD-I. We established an FDR threshold of 0.01 for genome-wide significance.<sup>27</sup>

#### Mouse Cortical Neuron Culture

Cortical neuronal cultures were generated from the brains of late embryos (E16.5–E17.5) of C57BL/6J wild-type mice. Pregnant mice were sacrificed by carbon dioxide euthanasia, more than 5 mouse embryos were decapitated, and soft bone fragments were removed to isolate the cortex from each hemisphere, and washed twice with pre-cooled neuron separation buffer (HBSS + 1  $\times$  Penicillin-Streptomycin [Gibco, #15140122]). The tissue blocks were then digested with 5 mL digestion buffer (Neurobasal [Gibco, #21103049] + 2 mg/ml Papain [Worthington, #LS003119] + 5 U/ml DNase I [SIGMA, #D4263-1VL]) at 37°C for 18 min (gently shook for every 6 min). After removal of the digestion buffer, the digested tissues were re-suspended with 1.5 ml neuron chow solution (Neurobasal [Gibco, #21103049] + 2% B27 [Gibco, #17504044] + 1  $\times$  GlutaMAX™-I [Gibco, #35050061], and 2.5% FBS [Biological Industries, #04-001-1ACS]). A sterilized pipette was used to dissociate tissues into single neuron cells by repeating pipetting. The single-cell suspension was allowed to rest for 3 min before the supernatant was aspirated and then passed through a filter to further remove impurities to obtain a cell suspension for culture. Finally,  $7 \times 10^5$  cells/well (6-well plate) were seeded onto poly-D-lysine-coated (SIGMA, #P6407-5MG; 10  $\mu$ g/ml) glass coverslips in neuron culture medium (Neurobasal [Gibco, #21103049] + 2% B27 [Gibco, #17504044] + 1  $\times$  GlutaMAX™-I [Gibco, #35050061]). The neuron culture medium was changed after 4 h to further remove dead cells and cell debris. Neurons were cultured in a cell incubator at 37°C in a humidified environment of 5% CO<sub>2</sub>.

### Plasmid Transfection and Immunofluorescence Staining

The coding sequence of the NEK4 transcript ([ENST00000383721.8](#)) was cloned into the pLenti-CAG-IRES-GFP (Addgene, #69047) vector. To analyze neuronal arbor development, either plenti-NEK4-3 × flag or the plenti-CAG-IRES-GFP empty vector was co-transfected into cortical neurons DIV (day in vitro) 3 with VENUS using Lipofectamine 3000 (Invitrogen, Cat. No: L3000-01). Four days post-transfection, cultures were fixed with 4% paraformaldehyde and 4% sucrose at room temperature for 15 min. Post-fixation, cells were incubated overnight at 4°C with primary antibodies, which included GFP (Abcam, #ab13970) for the control group and co-stained GFP (Abcam, #ab13970) with a flag (Cell Signaling Technology, #8146) for the NEK4-overexpression group. For the analysis of axon development, neurons seeded for 12 h were infected with lentiviruses expressing GFP in tandem with NEK4 or control. Neurons were fixed three days post-infection, and immunofluorescence was conducted using anti-Flag and anti-GFP antibodies for NEK4 overexpression and anti-GFP antibodies for the control at DIV (day in vitro) 4.

### Image Capture and Morphological Analyses

Images of transfected neurons were randomly selected and acquired using the 20× objective of the microscope. The Sholl analysis module in Fiji software ([Sholl Analysis \(imagej.net\)](#)) was used for neuronal arbors. Raw images were loaded and converted into 8-bit images in Fiji.<sup>28</sup> Subsequent steps, including drawing a fixed line from the soma center to the longest neurites and generating concentric rings, were conducted using the Sholl plugin. The number of neurite intersections against the radial distance from the soma center was quantified. Following previous studies, all Sholl analyses were carried out at 10 μm intervals up to a maximum radius of 500 μm.<sup>29</sup> A minimum of 30 cells were included per experiment, and all assays were performed in at least two independent experiments. Axon length was measured using Neuron-J.

## Results

### PWAS Identifies Risk Proteins Associated With SCZ and BD-I

We performed PWASs by integrating pQTL data from the ROSMAP human DLPFC ( $N = 376$ ) and GWASs of SCZ and BD-I. We identified 42 PWS proteins for SCZ ([Supplementary table S1](#) and [figure 1a](#)) and 14 for BD-I ([Supplementary table S1](#) and [figure 1b](#)). Interestingly, 4 PWS risk genes (*NEK4*, *HARS2*, *SUGP1*, and *DUS2*) from the SCZ cohort also showed PWS associations with BD-I ([Supplementary table S1](#) and [Figure 1](#)), suggesting a significant correlation between the protein abundance of these 4 genes and both SCZ and BD-I.

### TWAS Verified the PWS Risk Gene *NEK4* for Both SCZ and BD-I

Following the identification of risk proteins for SCZ and BD-I through our PWAS, we performed eQTL-based TWASs by integrating eQTL data from the CommonMind human DLPFC and GWASs of SCZ and BD-I. We compared the results with those from the PWAS. In the TWAS, we identified 103 genes associated with SCZ ([Supplementary table S2](#)), and 24 genes associated with BD-I ([Supplementary table S3](#)). Among these, the transcriptome-wide significant (TWS) genes that are shared between SCZ and BD-I, as revealed by our analysis, comprise *NEK4*, *GLT8D1*, *HAPLN4*, *MCHR1*, *LOC388152*, *SFMBT1*, *DOC2A*, and *TMEM10*. Furthermore, our study found that 10 of the 42 PWS proteins for SCZ (namely *NEK4*, *ACE*, *CGREF1*, *CORO7*, *COX11*, *CYP7B1*, *DARS2*, *DOC2A*, *RGS6*, and *TYW5*), as identified in the ROSMAP dataset, were also present in the TWAS findings ([Supplementary table S2](#) and [figure 1c](#)). For BD-I, two PWS proteins (*ADD3* and *NEK4*) were supported by the TWAS ([Supplementary table S3](#) and [figure 1d](#)) (significant overlapping, binomial test  $P < .05$ ). Also, Fisher's exact tests indicated an excessive overlap between TWAS and PWAS findings ( $P < .05$ ). Importantly, the *NEK4* gene, which displayed significant proteome-wide associations with both SCZ and BD-I in brain proteomes, was also supported by eQTL-based TWAS, suggesting that it is a high-confidence gene with significant mRNA and protein expression associations with SCZ and BD-I.

### MR Analysis Verifies the Association of *NEK4* Protein and mRNA With SCZ and BD-I

Following the protein and expression support of *NEK4* in our PWAS/TWAS analysis, we next applied the MR framework using brain proteome data, which enabled us to investigate the genetically predicted effects of *NEK4* ([figure 2](#)). The analysis revealed that the levels of *NEK4* protein were positively associated with the risk of both SCZ and BD-I ( $P_{SCZ} = 6.36 \times 10^{-14}$ ,  $P_{BD-I} = 7.87 \times 10^{-8}$ ). Further extending our analysis to the transcriptome data, we found a similar pattern of association, with *NEK4* mRNA levels being significantly linked to the risk of SCZ and BD-I ( $P_{SCZ} = 6.21 \times 10^{-5}$ ,  $P_{BD-I} = 1.02 \times 10^{-9}$ ). This dual evidence from both proteome and transcriptome analyses strengthens the hypothesis that *NEK4* plays a crucial role in the etiology of SCZ and BD-I.

### Drug Target Prioritization

Guided by our integrative analysis framework, we singled out the brain pathogenic protein *NEK4* as a drug target for both disorders. Furthermore, based on DGIdb, *NEK4* emerged as a potential therapeutic target for an array of pharmaceutical compounds, including CHEMBL541400,

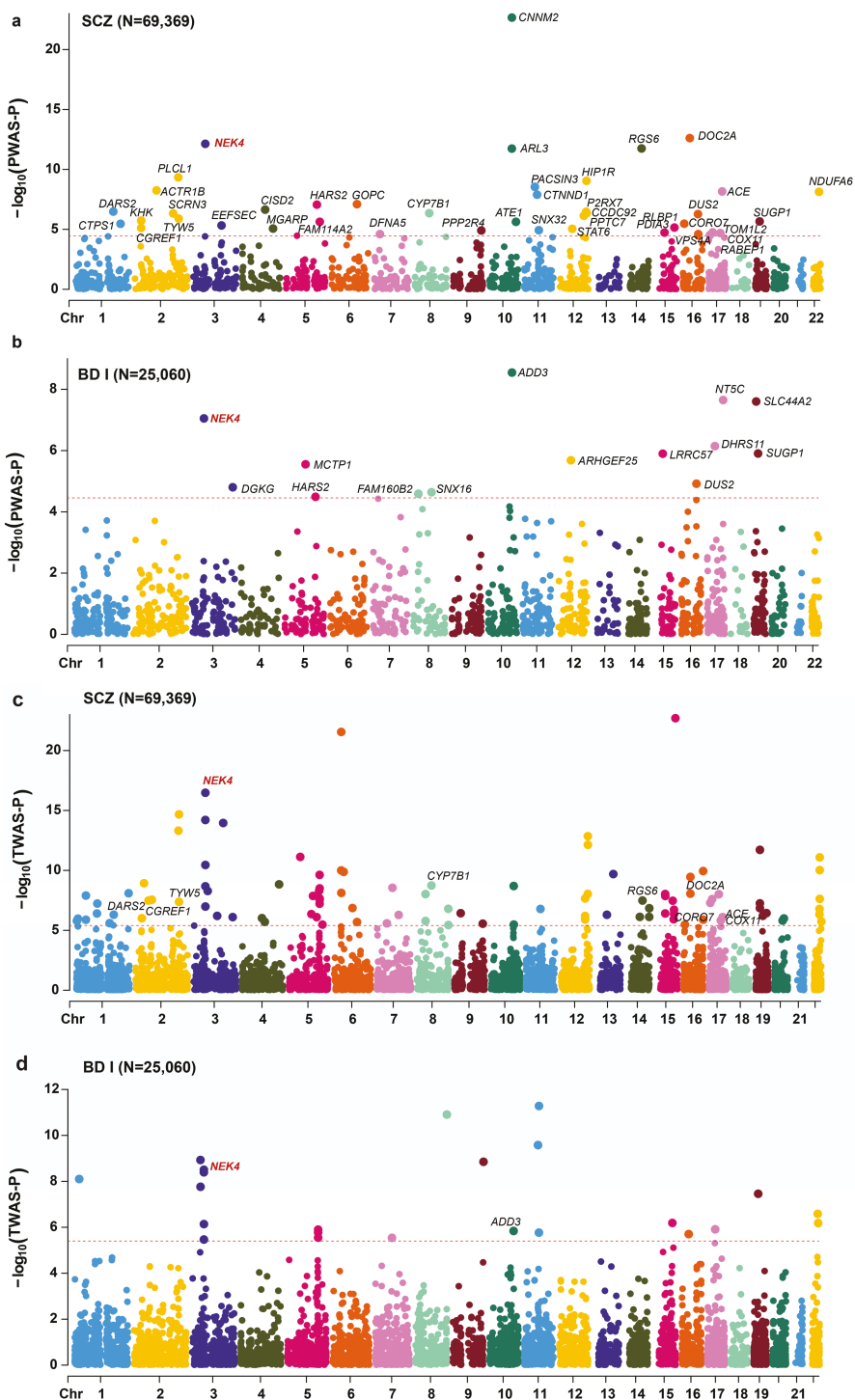


**Fig. 1.** Manhattan plots for the SCZ and BD-I PWAS in ROSMAP human brain proteomes and TWAS in COMMONMIND human brain transcriptomes. (a) Manhattan plot for the SCZ PWAS integrating the SCZ GWAS (69 369 cases and 236 642 controls) with the ROSMAP proteomes ( $N = 376$ ). (b) Manhattan plot for the BD-I PWAS integrating the BD-I GWAS (25 060 cases and 449 978 controls) with the ROSMAP proteomes ( $N = 376$ ). (c) Manhattan plot for the SCZ TWAS integrating the SCZ GWAS with the eQTL ( $N = 467$ ); Genes showing both eQTL-based TWS and PWS in SCZ are highlighted. (d) Manhattan plot for the BD-I TWAS integrating the BD-I GWAS with the eQTL ( $N = 467$ ); genes showing both eQTL-based TWS and PWS in BD-I are highlighted. Each dot on the circular axis represents a gene, and the association strength on the vertical axis represents the  $-\log_{10}(P)$  of PWAS and TWAS. The transcriptome-wide significance level in the COMMONMIND dataset was set at  $P < 3.95 \times 10^{-6}$  (adjusted by the Bonferroni multiple testing correction method). The proteome-wide significance level in the ROSMAP dataset was set at  $P < 3.5 \times 10^{-5}$  (adjusted by the Bonferroni multiple testing correction method). Genes showing TWS and PWS in SCZ or BD-I are distinctly marked. BD-I, bipolar I disorder; GWAS, genome-wide association study; PWAS, proteome-wide association studies; PWS, proteome-wide significant; SCZ, schizophrenia; TWAS, transcriptome-wide association studies; TWS, transcriptome-wide significant.

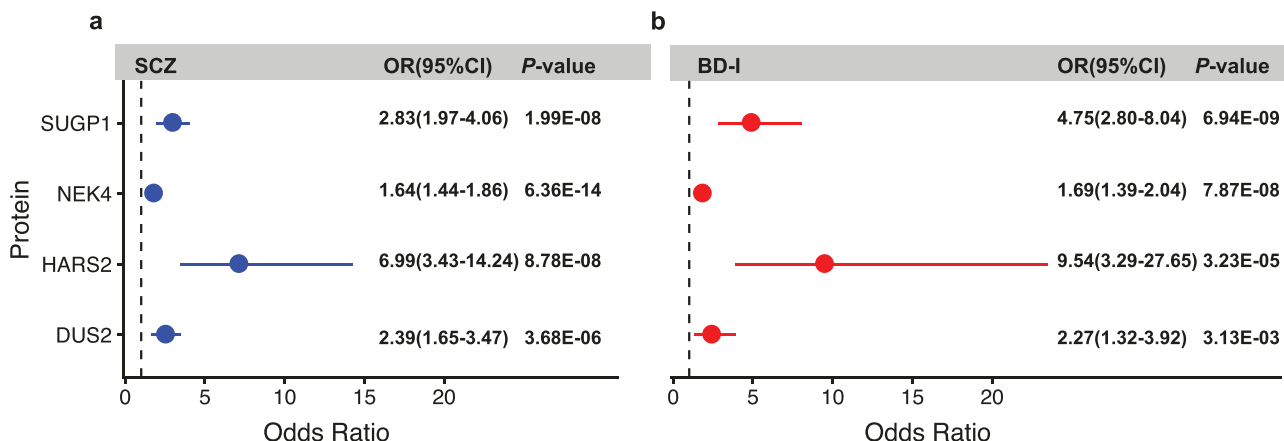


**Fig. 2.** MR analysis verified candidate genes in brain proteomes associated with SCZ and BD-I. (a) Verification of genes in SCZ, whereas (b) denotes genes in BD-I. This figure shows the OR and *P* values for the MR. BD-I, bipolar I disorder; SCZ, schizophrenia.

SNS-314, CHEMBL225519, GW441756X, CYC-116, DOVITINIB, CENISERTIB, ILORASERTIB, SP-600125, and R-406.

#### PleioFDR Analysis Supports Genetic Risk Loci Mapped to NEK4 for SCZ and BD-I

Through our pleioFDR analysis, we identified 266 significant SNPs ( $P < .01$ ) linked to genomic regions associated with both SCZ and BD-I (figure 3a and Supplementary table S4). We observed substantial evidence at rs11720243 ( $p\text{FDR} = 3.30 \times 10^{-6}$ ) as an overlapping locus for SCZ and BD-I (figure 3b and Supplementary table S4). SNP enrichment for SCZ in conjunction with BD-I, and vice versa, was indicated by stratified conditional Quantile-Quantile ( $Q$ - $Q$ ) plots (Supplementary figure S1), implying a polygenic overlap. In addition, pleioFDR analysis, in conjunction with DLPFC eQTL datasets and GWAS related to general cognitive function<sup>30</sup> and intelligence,<sup>31</sup> reiterated the essential roles of the *NEK4* gene for SCZ and BD-I related to cognition phenotypes. Detailed information on cognitive function and intelligence GWAS, as well as brain eQTL datasets, can be found in the Supplementary material. In the BrainSeq Phase 1 dataset,<sup>32</sup> the risk T-allele for SCZ and BD-I was associated with higher *NEK4* mRNA levels in DLPFC tissues (2-tailed  $P = 1.29 \times 10^{-10}$ ), with a similar association trend in the DLPFC in the BrainSeq Phase 2 dataset<sup>33</sup> (2-tailed  $P = 8.41 \times 10^{-27}$ , figure 3c) and in the GTEx dataset (2-tailed  $P = .04$ ). By employing HaploReg and leveraging data from the 1000 Genomes Project, we were able to identify 55 SNPs tagged with rs11720243 that significantly regulate *NEK4* expression in the DLPFC, as indicated by the selected eQTL dataset (Supplementary table S5). Moreover, the risk T-allele of rs11720243 was associated with poor cognitive abilities<sup>30</sup> ( $P = 9.15 \times 10^{-9}$ , figure 3b) and lower scores on intelligence tests<sup>31</sup> ( $P = 2.77 \times 10^{-10}$ , figure 3b). These findings collectively suggest an association between genetic variations in the

3p21.1 region and *NEK4* gene expression in the brain, potentially implicating this gene in the pathogenesis of SCZ and BD-I.

#### Cell-type Specific Analysis in the Human Brain

We next investigate cell-type enrichment of the risk gene using the human single-cell RNA-sequencing data (<https://portal.brain-map.org/atlas-and-data/rnaseq>) from the Cell Types dataset.<sup>19</sup> Significantly, we found that *NEK4* showed expression in glutamatergic neurons (figure 4).

#### NEK4 Promotes Dendritic Arborization and Axon Length

In our study, neurons overexpressing *NEK4* exhibited increased dendritic complexity compared to controls. This was quantified using Sholl analysis, which measures the number of neuronal branches intersecting concentric circles of increasing radius in 10  $\mu\text{m}$  increments (figure 5). In addition, primary mouse cortical neuron infection with *NEK4* or control lentivirus and immunofluorescence with anti-Flag antibody three days later confirmed the overexpression of *NEK4* in the neurons (Supplementary figure S2). Our results indicate that axons in the *NEK4* overexpression group were significantly longer than those in the control group (figure 5).

#### Discussion

In the course of this study, we identified 4 PWS genes (*NEK4*, *HARS2*, *SUGP1*, and *DUS2*) with protein abundance levels in the human brain showing significant association with SCZ and BD-I. We further endorsed *NEK4* as a risk factor for SCZ and BD-I using TWAS, MR, and pleioFDR analyses. These analyses demonstrate that the *NEK4* gene contributes to the neurophysiological underlying these two psychiatric disorders. Additionally,

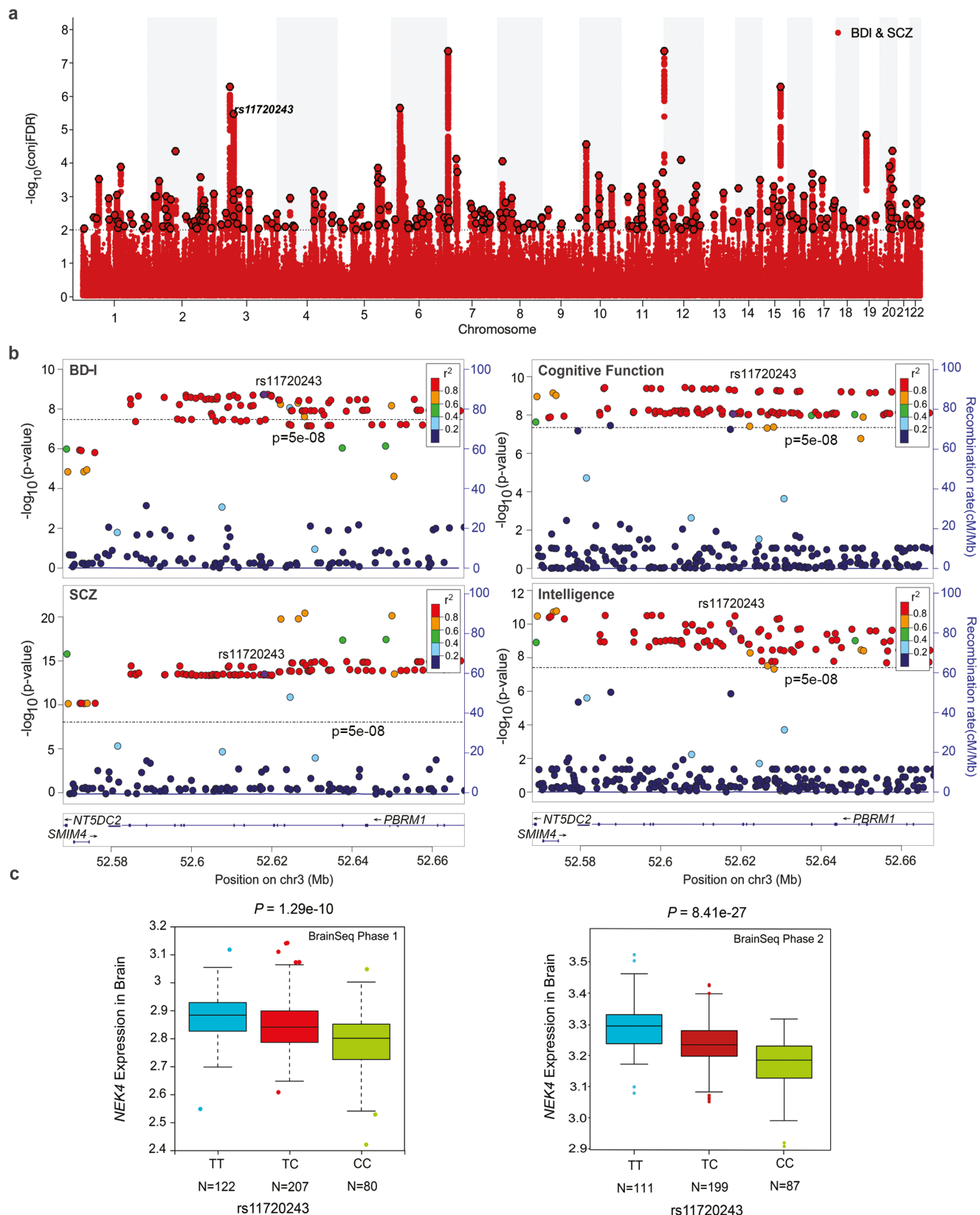


**Fig. 3.** Genetic overlaps between SCZ and BD-I. (a) Manhattan plot provides the association results for single marker analysis of SCZ and BD-I genetic overlap. (b) Association of psychiatric risk SNPs with general cognitive function and intelligence. A physical map of the region is given and depicts known genes within the region, and the LD is defined based on the SNP rs11720243. (c) Association of rs11720243 with NEK4 expression in the DLPFC in the BrainSeq Phase 1 dataset and in the BrainSeq Phase 2 dataset. BD-I, bipolar I disorder; SCZ, schizophrenia.

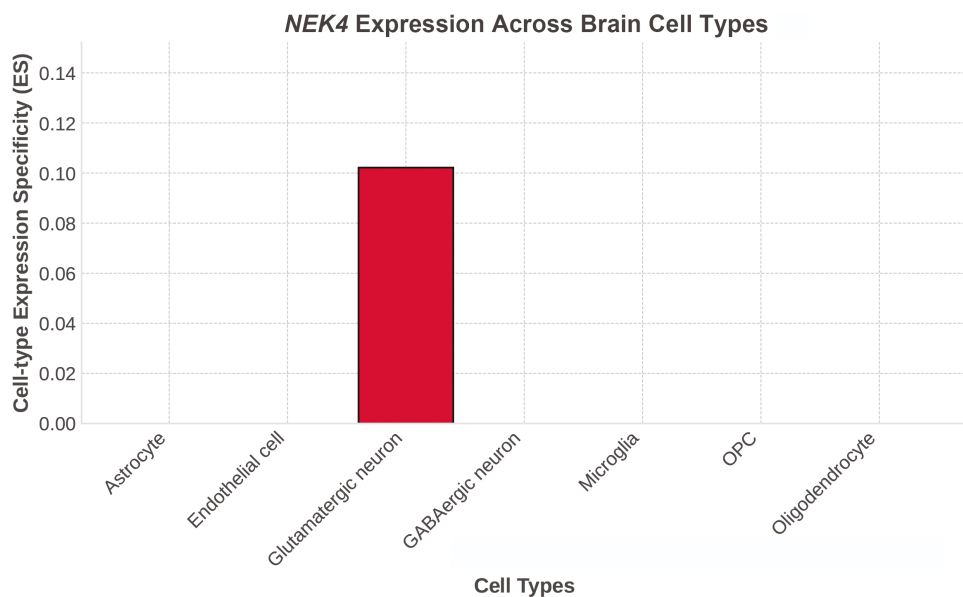


**Fig. 4.** Single-cell-type expression of the potential risk genes. Bar graph of single-cell-type enrichment for the risk gene. The diagram depicts CELL-type EXpression specificity (y-axis) for the risk gene (x-axis), with evidence of substantial enrichment within a specific brain cell type (histogram of the bar). OPC, oligodendrocyte precursor cell.

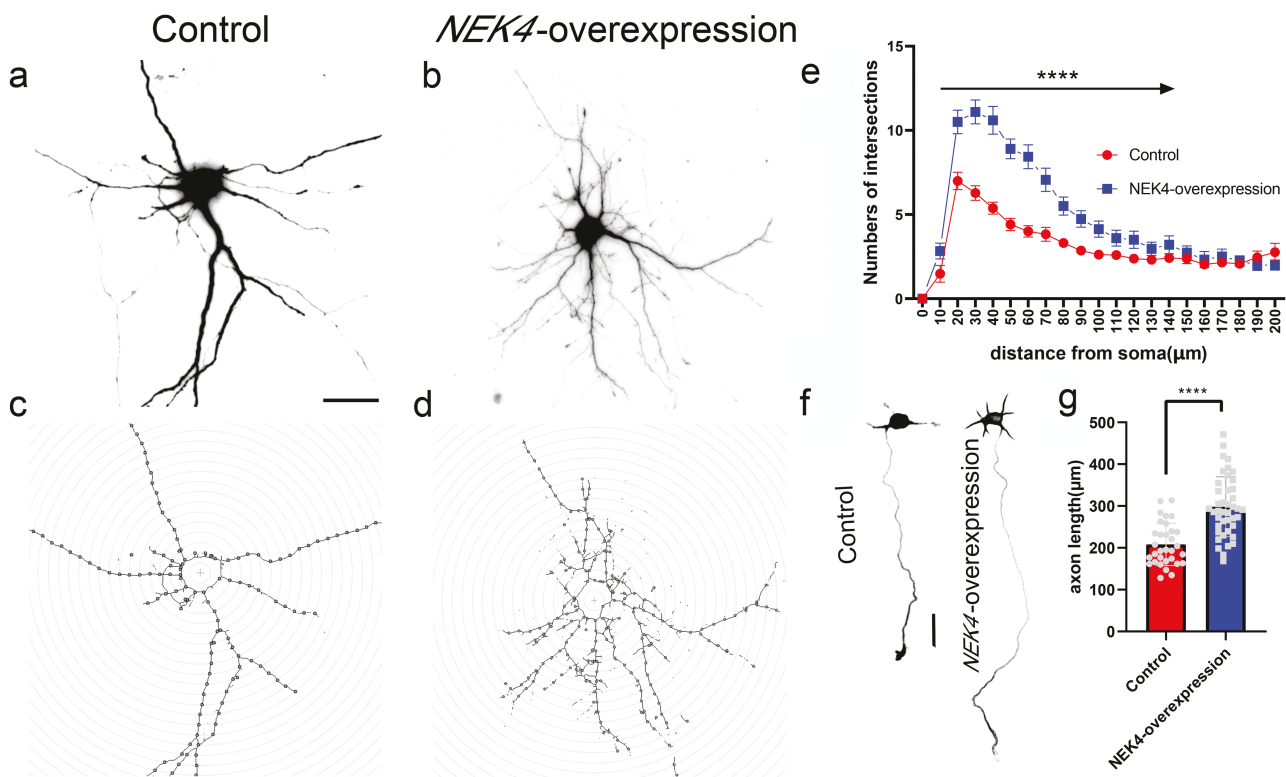


**Fig. 5.** NEK4 regulates neuronal development. (a–d) Representative images of cortical neurons transfected with control (plenti-CAG-IRES-GFP) or NEK4 overexpression vectors at DIV4 and fixed at DIV8. Only the GFP channel was shown to outline neuronal morphology (scale bar: 50  $\mu$ m). (e) Quantification of neuron complexity by Sholl analysis is described in (c) and (d). Two-tailed *t*-tests were applied to analyze the number of intersections of 10–150  $\mu$ m from the soma ( $F(29, 28) = 4.168$ ,  $t = 5.665$ ,  $df = 57$ ,  $P < .001$ ). (f) Representative pictures of cortical neurons infected with lentivirus expressing control (plenti-CAG-IRES-GFP) or NEK4 at DIV0.5 and fixed at DIV4. Only GFP is shown (scale bar: 20  $\mu$ m), and (g) quantification of the axon length with 2-tailed *t*-tests ( $F(41, 31) = 2.014$ ,  $t = 6.083$ ,  $df = 72$ ,  $P < 0.001$ ). Error bars indicate the standard error of the mean (SEM), \*\*\* $P < .0001$ ,  $N \geq 25$  neurons per condition.

we discovered that *NEK4* is primarily expressed in glutamatergic neurons and promotes dendritic branching and axon length in cultured primary neurons. These insights could be crucial for enhancing our understanding of potential treatment targets for SCZ and BD-I.

*NEK4*, one of the largest members of the NEK family, is implicated in the DNA damage response.<sup>34</sup> It has also been associated with psychiatric disorders based on convergent evidence. For instance, while the GWAS and integrative analyses focusing on SCZ and BD-I conducted by Gedik et al<sup>35</sup> and Liu et al's<sup>36</sup> differ from our approach, there is a consensus regarding the impact of *NEK4* on psychiatric disorders. Gedik et al<sup>35</sup> employed transcriptomic, proteomic, and methylomic analyses across blood and brain tissues to identify risk genes associated with neuropsychiatric and substance use disorders. In contrast, our study technique integrates MR, TWAS, and PWAS. This method was applied to analyze the most comprehensive SCZ GWAS dataset, with a particular focus on the shared biology between BD-I and SCZ. Additionally, our approach diverges from that of Liu et al,<sup>36</sup> as they examined separate GWAS datasets for psychiatric disorders and utilized MR on a specific set of 1263 functional proteins. Our findings not only corroborate but also expand upon the research conducted by Gedik and Liu et al, to identify *NEK4* as being associated with brain-specific signaling in both SCZ and BD-I. In earlier work, we found that the 3p21.1 mental risk allele, present in a state of low-to-high linkage disequilibrium, predicts elevated *NEK4* mRNA expression and diminished cognitive function in humans.<sup>8</sup> Building upon this, our current study utilized pleiotropy-informed conditional false discovery rate (pleioFDR) methods to explore the genetic overlap between SCZ and BD-I. Further evidence of rs11720243 (pFDR =  $3.30 \times 10^{-6}$ ) was provided, indicating it as an overlapping SNP for SCZ and BD-I. Our data showed that the risk T-allele of rs11720243 for SCZ and BD-I is associated with higher *NEK4* mRNA levels in both the BrainSeq Phase 1 dataset<sup>32</sup> and the BrainSeq Phase 2 dataset.<sup>33</sup> Furthermore, the risk T-allele of rs11720243 is linked to poorer cognitive performance<sup>30</sup> and lower intelligence test scores.<sup>31</sup> These findings demonstrate a connection between genetic variations at 3p21.1 and *NEK4* gene expression in the brain, suggesting a potential role for this gene in the etiology of SCZ and BD-I.

We previously found that manipulating the expression of *NEK4* gene, which is associated with a higher genetic risk, reduces the density of mushroom dendritic spines in primary cortical neurons.<sup>8</sup> This mirroring the spine pathology observed in the prefrontal cortex of psychiatric patients.<sup>37</sup> According to a study by Yao et al,<sup>38</sup> several genome-wide signals from the BD GWAS were driven by genetically regulated expression, with *NEK4* accounting for 90.1% of the GWAS signal. Furthermore, Li et al<sup>39</sup> confirmed a genetic susceptibility locus on 3p21.1, which includes the multigenetic region

*NEK4-ITI1-ITI1H3-ITI1H4*, in 65 Han Chinese SCZ families using whole-exome sequencing. Our results demonstrated a higher abundance of *NEK4* protein in both SCZ and BD-I, suggesting it is a potential target for future mechanistic and therapeutic studies.

Intriguingly, we found that overexpressing *NEK4* promotes dendritic arborization and axon length, implying its potential role in neurite and axon formation and the maintenance of dendritic spines. Additionally, we are aware of the fact that the processes of dendritic growth and dendritic spine development are distinct. The latter is a very dynamic process regulated by key synaptic proteins and other external stimuli. For example, the morphology of dendritic spines has obvious rhythm changes throughout the day.<sup>40</sup> Homer1 is an important scaffold protein for excitatory postsynaptic, one of its isoforms, Homer1a, regulates the remodeling of forebrain postsynaptic density during the wake/sleep cycle by moving into and out of postsynaptic PSD.<sup>41</sup> While the cytoskeleton is crucial for both the development of dendritic spines and the growth of neuron dendrites, the process of actin polymerization is crucial for dendritic spine production, whereas actin depolymerization promotes neurite outgrowth.<sup>42</sup> Nevertheless, there are numerous instances of genes exerting simultaneous effects on dendritic arborization and spine density, and these effects are not always the same direction.<sup>43-47</sup>

In addition to finding a significant link between *NEK4* protein abundance in the human brain and to SCZ and BD-I at the proteome level, we also discovered that *NEK4* was linked to SCZ and BD-I at the transcriptome level in the TWAS. This suggests that the gene has a similar neurophysiological basis in these two psychiatric disorders. *NEK4* at 3p21.1 was consistently and significantly important across virtually all eQTL datasets, despite the fact that the genome-wide lead risk genes discovered using several eQTL datasets differed considerably.<sup>8,48-50</sup> This outcome reinforces the validity of our TWAS findings. Furthermore, we identified four proteins shared between SCZ and BD-I, primarily enriched on the surface of glutamatergic neurons, further suggesting that *NEK4* is the genetic basis for the excitatory-inhibitory imbalance shared by SCZ and BD-I. This aligns with previous studies finding abnormal glutamate receptors, associated with psychomotor agitation.<sup>51</sup> Hence, we propose that *NEK4* might play a key role in ameliorating similar clinical symptoms and cognitive impairment in SCZ and BD-I.

To determine whether the proteins discovered in this study might be therapeutic targets, we prioritized *NEK4* as a potential therapeutic target for an array of pharmaceutical compounds including CHEMBL541400, SNS-314, CHEMBL225519, GW441756X, CYC-116, DOVITINIB, CENISERTIB, ILORASERTIB, SP-600125, and R-406. Additionally, a recent study showed that rs73078847 of *NEK4* was related to clozapine

levels ( $\beta = -.07$ ,  $P = 2.51 \times 10^{-4}$ , [Supplementary table S6](#)) in a group of 2989 patients with treatment-resistant SCZ.<sup>52</sup> These data suggest that *NEK4* may have the potential for mechanistic studies and future therapeutic development.

In our study, we have identified HARS2, SUGP1, and DUS2 as potential cross-disease therapeutic targets for SCZ and BD-I, extending our focus beyond *NEK4*. Previous genome-wide association studies have shown associations of HARS2<sup>53</sup> and SUGP1<sup>53</sup> with BD, while DUS2<sup>54</sup> has been linked to SCZ. Our findings support the involvement of these genes at the protein level in both SCZ and BD-I. Notably, HARS2, SUGP1, and DUS2 appear to play roles in critical biological pathways. These include pathways associated with excitatory neurons, mitochondrial function,<sup>55</sup> and tRNA post-transcriptional modification.<sup>56</sup> Such mechanisms have been extensively explored in studies of SCZ and BD-I, highlighting their significance in the pathology of these neuropsychiatric disorders. The discovery of these genes and their implicated pathways offers valuable insights into the shared mechanisms underlying SCZ and BD-I.

We have identified several key considerations for interpreting our findings: Firstly, while pQTL and eQTL analyses are informative for interpreting GWAS signals, they represent a partial view of the genetic intricacies of SCZ and BD-I. A more holistic understanding necessitates investigations that extend to epigenetics, including mQTL studies, single-cell sequencing, and comprehensive whole-genome analysis. Secondly, our study's proteome coverage was not exhaustive, raising the possibility that we missed proteins critical to these conditions. Future research should broaden proteome analysis and employ novel detection methods to identify additional associations. Thirdly, variability in GWAS sample sizes and the statistical limitations of xQTL methods have curtailed our ability to discern subtle genetic associations, underscoring the necessity for enhanced methodologies and greater availability of individual genetic data. Finally, elucidating the causal roles of proteins associated with SCZ and BD-I is crucial for the development of targeted treatments.

In conclusion, we identified that abnormal protein levels of *NEK4* are associated with shared genetic risk between SCZ and BD-I. Given the substantial similar/overlapping symptoms between patients with schizophrenia and patients with BD-I, as well as the known diagnostic shifts following the first admission for psychosis, the two disorders likely have shared pathology and aetiological mechanisms. Our data thus suggest that *NEK4* may be involved in the overlapping pathogenesis, potentially through its impact on dendritic arborization and axon length, and dendritic spine morphogenesis. As such, it may serve as a potential target for future mechanistic studies of the two psychiatric disorders and offers novel insights for potential therapeutic target identification.

## Supplementary Material

Supplementary material is available at <https://academic.oup.com/schizophreniabulletin/>.

## Acknowledgments

The data available in the AD Knowledge Portal would not be possible without the participation of research volunteers and the contribution of data by collaborating researchers. We thank the participants of the ROS, MAP, Mayo, Mount Sinai Brain Bank and Banner Sun Health Research Institute Brain and Body Donation Program for their time and participation. Data were generated as part of the CommonMind Consortium supported by funding from Takeda Pharmaceuticals Company Limited, F. Hoffman-La Roche Ltd. and NIH grants R01MH085542, R01MH093725, P50MH066392, P50MH080405, R01MH097276, R01-MH-075916, P50M096891, P50MH084053S1, R37MH057881 and R37MH057881S1, HHSN271201300031C, AG02219, AG05138 and MH06692. Brain tissue for the study was obtained from the following brain bank collections: the Mount Sinai NIH Brain and Tissue Repository, the University of Pennsylvania Alzheimer's Disease Core Center, the University of Pittsburgh NeuroBioBank and Brain and Tissue Repositories and the NIMH Human Brain Collection Core. CMC Leadership: Pamela Sklar, Joseph Buxbaum (Icahn School of Medicine at Mount Sinai), Bernie Devlin, David Lewis (University of Pittsburgh), Raquel Gur, Chang-Gyu Hahn (University of Pennsylvania), Keisuke Hirai, Hiroyoshi Toyoshiba (Takeda Pharmaceuticals Company Limited), Enrico Domenici, Laurent Essioux (F. Hoffman-La Roche Ltd), Lara Mangravite, Mette Peters (Sage Bionetworks), Thomas Lehner, Barbara Lipska (NIMH).

The authors declare no competing interests.

## Funding

This work was partly funded by the National Natural Science Foundation of China Key Project (T.L., and P.S., 81920108018); the National Natural Science Foundation of China Project (C.Z., 82001413); the Key R & D Program of Zhejiang (T.L. 2022C03096); Project for Hangzhou Medical Disciplines of Excellence and Key Project for Hangzhou Medical Disciplines (T.L. 202004A11); Postdoctoral Foundation of West China Hospital (C.Z., 2020HXBH163); Spring City Plan: the High-level Talent Promotion and Training Project of Kunming (M.L., 2022SCP001); and in part by grants from Nanhu Brain-computer Interface Institute. Xiao Xiao was also supported by the CAS "Light of West China" Program, CAS Youth Innovation Promotion Association, and Yunnan Revitalization Talent Support Program Young Talent Project.

## Ethical approval

This study involves animal subjects and was approved by the Animal Ethic Committee of Kunming Institute of Zoology prior to the study (IACUC-RE-2021-11-001). The study's use of publicly available data that included human subjects was ethical.

## Author contributions

CCZ and TL designed the experiment. CCZ and PKS performed the PWAS, cell-type specificity analysis, pleioFDR analysis and TWAS. ZHY, ML, and XX performed the neuronal experiments. CCZ, QW, WJG, LXJ, and WD performed the MR analysis. All authors contributed to, reviewed, and approved the final draft of the paper. All authors had full access to all the data in the study and had final responsibility for the decision to submit for publication.

## Data Availability

Summary statistics of the GWAS for SCZ and BD-I can be obtained from the Psychiatric Genomics Consortium at <https://pgc.unc.edu/>. The ROSMAP study's brain eQTL and pQTL data are publicly accessible at the following links: eQTL data at <https://www.synapse.org/#/Synapse:syn17015233> and pQTL data at <https://www.synapse.org/#/Synapse:syn23245229>. Cell-type specificity data are available at <https://portal.brain-map.org/atlas-and-data/rnaseq>.

## Code Availability

For the CELLEX analysis, we utilized the tool available at <https://github.com/perslab/CELLEX>, adhering to the recommended normalization method and preprocessing steps. The FUSION source code, used in our analysis, can be found at <http://gusevlab.org/projects/fusion>. The source code for the MR analysis is available at <https://mrcieu.github.io/TwoSampleMR/>. We also provide other custom codes on GitHub ([https://github.com/zhangcc89claire/Code\\_for\\_Sb](https://github.com/zhangcc89claire/Code_for_Sb)).

## References

- Collins PY, Patel V, Joestl SS, et al; Scientific Advisory Board and the Executive Committee of the Grand Challenges on Global Mental Health. Grand challenges in global mental health. *Nature*. 2011;475(7354):27–30.
- Bipolar Disorder Schizophrenia Working Group of the Psychiatric Genomics Consortium. Genomic dissection of bipolar disorder and schizophrenia, including 28 subphenotypes. *Cell*. 2018;173(7):1705–1715 e1716.
- Mullins N, Forstner AJ, O'Connell KS, et al; HUNT All-In Psychiatry. Genome-wide association study of more than 40,000 bipolar disorder cases provides new insights into the underlying biology. *Nat Genet*. 2021;53(6):817–829.
- Upthegrove R, Marwaha S, Birchwood M. Depression and schizophrenia: cause, consequence, or trans-diagnostic issue? *Schizophr Bull*. 2017;43(2):240–244.
- American Psychiatric Association. Diagnostic and Statistical Manual of Mental Disorders(DSM-5®): American Psychiatric Pub; 2013. *J Physiother Res Salvador*. 2019;9(2):155–158.
- Kwentus J, Riesenber RA, Marandi M, et al. Rapid acute treatment of agitation in patients with bipolar I disorder: a multicenter, randomized, placebo-controlled clinical trial with inhaled loxapine. *Bipolar Disord*. 2012;14(1):31–40.
- Pompili M, Ducci G, Galluzzo A, Rosso G, Palumbo C, De Berardis D. The management of psychomotor agitation associated with schizophrenia or bipolar disorder: a brief review. *Int J Environ Res Public Health*. 2021;18(8):4368.
- Yang Z, Zhou D, Li H, et al. The genome-wide risk alleles for psychiatric disorders at 3p21.1 show convergent effects on mRNA expression, cognitive function, and mushroom dendritic spine. *Mol Psychiatry*. 2020;25(1):48–66.
- Ren H, Meng Y, Zhang Y, et al. Spatial expression pattern of ZNF391 gene in the brains of patients with schizophrenia, bipolar disorders or major depressive disorder identifies new cross-disorder biotypes: a trans-diagnostic, top-down approach. *Schizophr Bull*. 2021;47(5):1351–1363.
- Xiao X, Zhang C, Grigoriu-Serbanescu M, et al. The cAMP responsive element-binding (CREB)-1 gene increases risk of major psychiatric disorders. *Mol Psychiatry*. 2018;23(9):1957–1967.
- Wingo AP, Dammer EB, Breen MS, et al. Large-scale proteomic analysis of human brain identifies proteins associated with cognitive trajectory in advanced age. *Nat Commun*. 2019;10(1):1619.
- Timp W, Timp G. Beyond mass spectrometry, the next step in proteomics. *Sci Adv*. 2020;6(2):eaax8978.
- Rolland DCM, Basrur V, Jeon Y-K, et al. Functional proteogenomics reveals biomarkers and therapeutic targets in lymphomas. *Proc Natl Acad Sci USA*. 2017;114(25):6581–6586.
- Wingo AP, Liu Y, Gerasimov ES, et al. Integrating human brain proteomes with genome-wide association data implicates new proteins in Alzheimer's disease pathogenesis. *Nat Genet*. 2021;53(2):143–146.
- Wingo TS, Liu Y, Gerasimov ES, et al. Brain proteome-wide association study implicates novel proteins in depression pathogenesis. *Nat Neurosci*. 2021;24(6):810–817.
- Liu J, Li X, Luo XJ. Proteome-wide association study provides insights into the genetic component of protein abundance in psychiatric disorders. *Biol Psychiatry*. 2021;90(11):781–789.
- Trubetskoy V, Pardiñas AF, Qi T, et al. Mapping genomic loci implicates genes and synaptic biology in schizophrenia. *Nature*. 2022;604(7906):502–508.
- Gusev A, Ko A, Shi H, et al. Integrative approaches for large-scale transcriptome-wide association studies. *Nat Genet*. 2016;48(3):245–252.
- Ou Y-N, Yang Y-X, Deng Y-T, et al. Identification of novel drug targets for Alzheimer's disease by integrating genetics and proteomes from brain and blood. *Mol Psychiatry*. 2021;26(10):6065–6073.
- Wang M, Beckmann ND, Roussos P, et al. The Mount Sinai cohort of large-scale genomic, transcriptomic and proteomic data in Alzheimer's disease. *Sci Data*. 2018;5(1):1–16.
- Davey Smith G, Hemani G. Mendelian randomization: genetic anchors for causal inference in epidemiological studies. *Hum Mol Genet*. 2014;23(R1):R89–R98.

22. Rasooly D, Patel CJ. Conducting a reproducible Mendelian randomization analysis using the R analytic statistical environment. *Curr Protoc Hum Genet*. 2019;101(1):e82.

23. Hemani G, Zheng J, Elsworth B, et al. The MR-Base platform supports systematic causal inference across the human genome. *Elife*. 2018;7:e34408.

24. Fromer M, Roussos P, Sieberts SK, et al. Gene expression elucidates functional impact of polygenic risk for schizophrenia. *Nat Neurosci*. 2016;19(11):1442–1453.

25. Timshel PN, Thompson JJ, Pers TH. Genetic mapping of etiologic brain cell types for obesity. *Elife*. 2020;9:e55851.

26. Freshour SL, Kiwala S, Cotto KC, et al. Integration of the Drug-Gene Interaction Database (DGIdb 4.0) with open crowdsource efforts. *Nucleic Acids Res*. 2021;49(D1):D1144–D1151.

27. Andreassen OA, Thompson WK, Schork AJ, et al; Psychiatric Genomics Consortium (PGC). Improved detection of common variants associated with schizophrenia and bipolar disorder using pleiotropy-informed conditional false discovery rate. *PLoS Genet*. 2013;9(4):e1003455.

28. Schindelin J, Arganda-Carreras I, Frise E, et al. Fiji: an open-source platform for biological-image analysis. *Nat Methods*. 2012;9(7):676–682.

29. Binley KE, Ng WS, Tribble JR, Song B, Morgan JE. Sholl analysis: a quantitative comparison of semi-automated methods. *J Neurosci Methods*. 2014;225:65–70.

30. Lee JJ, Wedow R, Okbay A, et al; 23andMe Research Team. Gene discovery and polygenic prediction from a 1.1-million-person GWAS of educational attainment. *Nat Genet*. 2018;50(8):1112–1121.

31. Savage JE, Jansen PR, Stringer S, et al. Genome-wide association meta-analysis in 269,867 individuals identifies new genetic and functional links to intelligence. *Nat Genet*. 2018;50(7):912–919.

32. Jaffe AE, Straub RE, Shin JH, et al; BrainSeq Consortium. Developmental and genetic regulation of the human cortex transcriptome illuminate schizophrenia pathogenesis. *Nat Neurosci*. 2018;21(8):1117–1125.

33. Collado-Torres L, Burke EE, Peterson A, et al; BrainSeq Consortium. Regional heterogeneity in gene expression, regulation, and coherence in the frontal cortex and hippocampus across development and schizophrenia. *Neuron*. 2019;103(2):203–216.e8.

34. Peres de Oliveira A, Kazuo Issayama L, Betim Pavan IC, et al. Checking NEKs: overcoming a bottleneck in human diseases. *Molecules*. 2020;25(8):1778.

35. Gedik H, Nguyen TH, Peterson RE, et al. Identifying potential risk genes and pathways for neuropsychiatric and substance use disorders using intermediate molecular mediator information. *Front Genet*. 2023;14:1191264.

36. Liu J, Cheng Y, Li M, Zhang Z, Li T, Luo X-J. Genome-wide Mendelian randomization identifies actionable novel drug targets for psychiatric disorders. *Neuropsychopharmacology*. 2023;48(2):270–280.

37. Penzes P, Cahill ME, Jones KA, VanLeeuwen JE, Woolfrey KM. Dendritic spine pathology in neuropsychiatric disorders. *Nat Neurosci*. 2011;14(3):285–293.

38. Yao S, Wu H, Liu T-T, et al. Epigenetic element-based transcriptome-wide association study identifies novel genes for bipolar disorder. *Schizophr Bull*. 2021;47(6):1642–1652.

39. Li M, Shen L, Chen L, et al. Novel genetic susceptibility loci identified by family based whole exome sequencing in Han Chinese schizophrenia patients. *Transl Psychiatry*. 2020;10(1):5.

40. De Vivo L, Bellesi M, Marshall W, et al. Ultrastructural evidence for synaptic scaling across the wake/sleep cycle. *Science*. 2017;355(6324):507–510.

41. Diering GH, Nirujogi RS, Roth RH, Worley PF, Pandey A, Huganir RL. Homer1a drives homeostatic scaling-down of excitatory synapses during sleep. *Science*. 2017;355(6324):511–515.

42. Zhang S-X, Duan L-H, Qian H, Yu X. Actin aggregations mark the sites of neurite initiation. *Neurosci Bull*. 2016;32:1–15.

43. Bonhoeffer T, Caroni P. *Structural Plasticity in Dendrites and Spines*. Dendrites: Oxford University Press; 2016:557.

44. Peng YR, He S, Marie H, et al. Coordinated changes in dendritic arborization and synaptic strength during neural circuit development. *Neuron*. 2009;61(1):71–84.

45. O'Neill K, Akum B, Dhawan S, Kwon M, Langhammer C, Firestein B. Assessing effects on dendritic arborization using novel Sholl analyses. *Front Cell Neurosci*. 2015;9:1–14.

46. Ji C, Tang Y, Zhang Y, et al. Glutaminase 1 deficiency confined in forebrain neurons causes autism spectrum disorder-like behaviors. *Cell Rep*. 2023;42(7):112712.

47. Teng L-L, Lu G-L, Chiou L-C, et al. Serotonin receptor HTR6-mediated mTORC1 signaling regulates dietary restriction-induced memory enhancement. *PLoS Biol*. 2019;17(3):e2007097.

48. Reay WR, Cairns MJ. Pairwise common variant meta-analyses of schizophrenia with other psychiatric disorders reveals shared and distinct gene and gene-set associations. *Transl Psychiatry*. 2020;10(1):134.

49. Li Y, Ma C, Li S, et al. Regulatory variant rs2535629 in ITIH3 intron confers schizophrenia risk by regulating CTCF binding and SFMBT1 expression. *Adv Sci*. 2022;9(6):e2104786.

50. Gusev A, Mancuso N, Won H, et al; Schizophrenia Working Group of the Psychiatric Genomics Consortium. Transcriptome-wide association study of schizophrenia and chromatin activity yields mechanistic disease insights. *Nat Genet*. 2018;50(4):538–548.

51. Shaltiel G, Maeng S, Malkesman O, et al. Evidence for the involvement of the kainate receptor subunit GluR6 (GRIK2) in mediating behavioral displays related to behavioral symptoms of mania. *Mol Psychiatry*. 2008;13(9):858–872.

52. Pardinas AF, Nalpantidis M, Pocklington AJ, et al. Pharmacogenomic variants and drug interactions identified through the genetic analysis of clozapine metabolism. *Am J Psychiatry*. 2019;176(6):477–486.

53. Li H-J, Zhang C, Hui L, et al; GeseDNA Research Team. Novel risk loci associated with genetic risk for bipolar disorder among Han Chinese individuals: a Genome-Wide Association Study and meta-analysis. *JAMA Psychiatry*. 2021;78(3):320–330.

54. Pardiñas AF, Holmans P, Pocklington AJ, et al; GERAD1 Consortium. Common schizophrenia alleles are enriched in mutation-intolerant genes and in regions under strong background selection. *Nat Genet*. 2018;50(3):381–389.

55. Gong S, Wang X, Meng F, et al. Overexpression of mitochondrial histidyl-tRNA synthetase restores mitochondrial dysfunction caused by a deafness-associated tRNA(His) mutation. *J Biol Chem*. 2020;295(4):940–954.

56. Bou-Nader C, Pecqueur L, Bregeon D, et al. An extended dsRBD is required for post-transcriptional modification in human tRNAs. *Nucleic Acids Res*. 2015;43(19):9446–9456.